Optical conductivity as a probe of a hidden Fermi-liquid behavior in $BaFe_{1.904}Ni_{0.096}As_2$*

Yang Yan-Xing(杨彦兴)[a)b)], Xiong Rui(熊 锐)[a)†], Fang Zhi-Hao(方之颢)[a)], Xu Bing(许 兵)[b)], Xiao Hong(肖 宏)[b)], Qiu Xiang-Gang(邱祥冈)[b)], Shi Jing(石 兢)[a)], and Wang Kai(王 凯)[b)‡]

[a)] School of Physics and Technology, Wuhan University, Wuhan 430072, China

[b)] Beijing National Laboratory for Condensed Matter Physics, National Laboratory for Superconductivity, Institute of Physics, Chinese Academy of Sciences, Beijing 100190, China

(Received 17 April 2014; revised manuscript received 28 May 2013; published online 10 August 2014)

We measured the infrared reflectivity of $BaFe_{1.904}Ni_{0.096}As_2$ single crystal from room temperature down to 20 K. Two Drude terms and a Lorentz term well describe the real part of the optical conductivity $\sigma_1(\omega)$. We fit the reciprocal of static optical conductivity $1/\sigma_1(0)$ by the power law $\rho(T)=\rho_0+AT^n$ with n=1.6. The "broad" Drude component exhibits an incoherent background with a T-independent scattering rate $1/\tau_b$, while the other "narrow" one reveals a T-quadratic scattering rate $1/\tau_n$, indicating a hidden Fermi-liquid behavior in $BaFe_{1.904}Ni_{0.096}As_2$ compound.

Keywords: iron-based superconductor, Fermi liquid, optical conductivity

PACS: 74.70.Xa, 72.15.–v, 78.30.–j **DOI:** 10.1088/1674-1056/23/10/107401

1. Introduction

In 2008 the discovery of superconductivity (SC) with T_c up to 55 K in iron pnictides[1–3] raised intense interest in their electronic properties. A similar phase diagram[4] with cuprates evolves more speculation of the links between these two categories of superconductors. However, it becomes apparent that iron pnictides are more complicated in the electronic properties than cuprates, where a single Cu–O hybridized band predominates at the Fermi surface, and different methods and band structures all lead to d-wave pairing.[5] Furthermore, cuprates are doped-Mott insulators with properties related to the effects of strong correlations in the narrow Cu 3d band, while iron pnictides are metallic systems with a spin density wave state at low doping.[6] Three hole bands and two electron bands traverse the Fermi level obtained by electronic structure calculations[7–9] and this is confirmed by angular resolved photoemission spectroscopy (ARPES).[10,11] A previous study has revealed two electronic subsystems coexisting in iron pnictides,[12] which is consistent with its multiple band character.

The Fermi-liquid description is one of the most successful theories in condensed-matter physics. It is proposed to describe the properties of Fermi systems at low temperature onto a dilute gas of strongly interacting fermionic excitations.[13] Deviations from Fermi-liquid behavior are widely discussed in iron pnictides. Non-Fermi-liquid (NFL) behaviors are possibly linked to the antiferromagnetic quantum critical point (QCP) and strong spin fluctuations, which may induce the pairing of electrons in high-T_c superconductors,[14–16] but systematic analyses of transport properties do not exhibit such a feature over the phase diagram.

Infrared (IR) spectroscopy is a powerful tool to study the charge carrier dynamics in strongly correlated systems.[17,18] High energy resolution, bulk sensitivity, and the existed sum rules make it equipped to get valuable information about the energy scale of electronic interactions and SC, charge density wave (CDW), and spin density wave (SDW).[19] In this paper, we study the normal state properties of $BaFe_{1.904}Ni_{0.096}As_2$ single crystal through infrared reflectivity. We find that there exists two electronic subsystems in this superconductor, which exhibits different characters with decreasing temperature. These observations suggest a multiple band character and a hidden Fermi-liquid behavior in $BaFe_{1.904}Ni_{0.096}As_2$.

2. Experiments

High quality $BaFe_{1.904}Ni_{0.096}As_2$ single crystals were grown by using the FeAs flux method. The resistivity of the crystal exhibits a sharp superconducting transition at T_c = 20.0 K. The near normal incidence reflectivity from 40 cm^{-1} to 7000 cm^{-1} of freshly cleaved sample was measured by using infrared Fourier transform spectrometers (Bruker Vertex 80v) at 12 different temperatures, ranging from 275 K down to 20 K. The *in situ* gold overfilling technique[20] was used to obtain the absolute reflectivity of the sample. In order to get the optical conductivity of the sample via the Kramers–Kronig relations, we extend the data to near infrared range,

*Project supported by the National Natural Science Foundation of China (Grant Nos. 11374345, 11104335, and 91121004) and the National Basic Research Program of China (Grant Nos. 2012CB821403, 2011CBA00107, and 2012CB921302).

†Corresponding author. E-mail: xiongrui@whu.edu.cn

‡Corresponding author. E-mail: wangkai@iphy.ac.cn

© 2014 Chinese Physical Society and IOP Publishing Ltd

visible range, and UV range by using the reflectivity of optimally doped $BaFe_{1.84}Co_{0.16}As_2$ compound at room temperature measured by using infrared Fourier transform spectrometers (Bruker IFS66v) and AvaSpec-2048 ×14 model fiber optic spectrometer.

3. Results and discussion

Figure 1 shows the optical reflectivity of $BaFe_{1.904}Ni_{0.096}As_2$ single crystal at selected temperatures in the infrared frequency range. In the normal state, the material exhibits a metallic response, which is characterized by a very high reflectivity at low frequencies and a tendency to approach unity at zero frequency. This exhibits clearly that the reflectivity $R(\omega)$ increases continuously at low frequency as the temperature cools, indicating a better metallicity at low temperatures. We cannot see any clear-cut plasma edge, as in parent compound of 122 iron pnictides.[21] A tiny phonon peak can be seen at about 250 cm^{-1}, which is widely discussed in the lattice dynamics of 122 iron pnictides.[22,23] The inset of Fig. 1 shows the reflectivity of the whole frequency range, which we measured at 275 K.

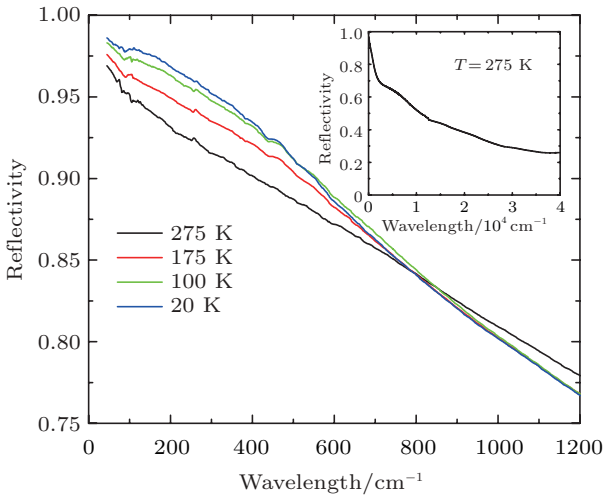


Fig. 1. (color online) Infrared reflectivity of $BaFe_{1.904}Ni_{0.096}As_2$ at selected temperatures. The inset shows the reflectivity of the whole frequency range measured from 45 cm^{-1} to 4×10^4 cm^{-1} at 275 K.

The real part of optical conductivity is derived from the reflectivity via the Kramers–Kronig analysis and is shown in Fig. 2 (thick solid lines). A Hagen–Rubens form ($R = 1-A\sqrt{\omega}$) is used for the low-frequency extrapolation. At high frequencies, $R(\omega)$ is assumed to be constant up to 40 eV, above which a free-electron response (ω^{-4}) is used. All of the spectra exhibits a well-known Drude-like metallic response.

In order to quantitatively analyze the optical conductivity, we fit $\sigma_1(\omega)$ to the Drude–Lorentz model,

$$\sigma_1(\omega) = \frac{2\pi}{Z_0}\sum_k \left[\frac{\Omega_{p,k}^2}{\tau_k(\omega^2+\tau_k^{-2})} + \frac{\gamma_k\omega^2 S_k^2}{(\Omega_k^2-\omega^2)^2+\gamma_k^2\omega^2}\right], \quad (1)$$

where Z_0 is the vacuum impedance. The first term in Eq. (1) describes a sum of the free-carrier Drude response, each of which is characterized by a plasma frequency $\Omega_p^2 = 4\pi ne^2/m^*$, where n is carrier concentration, m^* is effective mass, and $1/\tau$ is scattering rate. The second term corresponds to a sum of the Lorentz oscillators, characterized by a resonance frequency (ω_k), a line width (γ_k), and an oscillator strength (Ω_k).

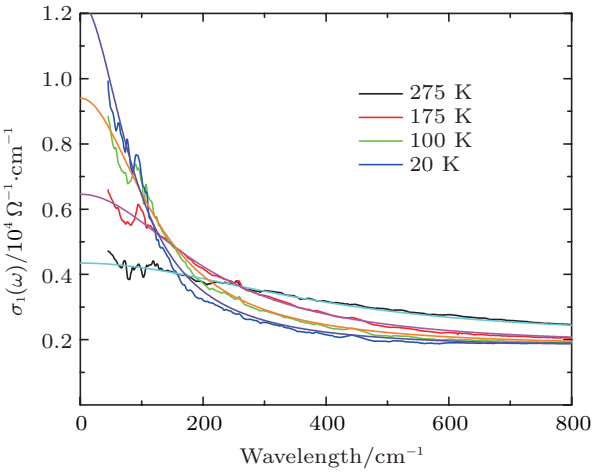


Fig. 2. (color online) Thick solid lines are *ab* plane $\sigma_1(\omega)$ of $BaFe_{1.904}Ni_{0.096}As_2$ at selected temperatures. The smooth thin lines through the data are fits with Drude–Lorentz model.

As shown in Fig. 3, $\sigma_1(\omega)$ at 275 K is well described by two Drude terms and a Lorentz term up to 8×10^3 cm^{-1}. The same fit at other temperatures is shown in Fig. 2 (thin smooth lines).

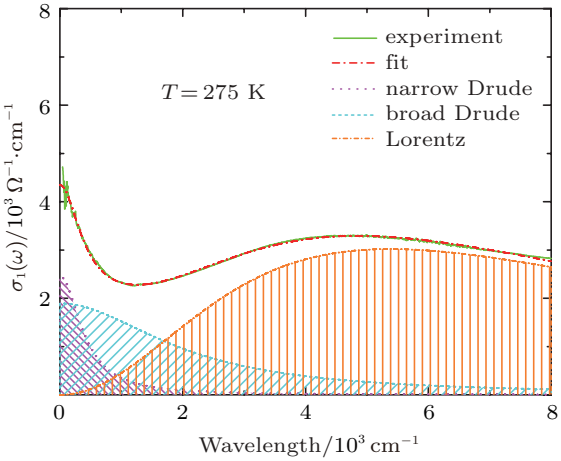


Fig. 3. (color online) The green solid curve is the measured $\sigma_1(\omega)$ of $BaFe_{1.904}Ni_{0.096}As_2$. The red dashed–dotted line through the data is the fit which is decomposed into a broad Drude term (cyan short dashed line), a narrow Drude term (magenta dotted line), and a Lorentz term (orange short dashed–dotted line).

Instead of using Matthiessen's rule, where different contributions of scattering are treated additively, we add up their contributions to the conductivity.[22] We extract the total resistivity $\rho_{total} = 1/(\sigma_n(0)+\sigma_b(0))$, where $\sigma_n(0)$ and $\sigma_b(0)$

are the value of narrow and broad Drude terms at zero frequency respectively, as equivalence of the dc resistivity. Figure 4 shows the ρ_{total} as a function of temperature, which is fitted by the power law

$$\rho(T) = \rho_0 + AT^n \tag{2}$$

with $n = 1.6$ which is inconsistent with the result of the transport measurements. A quadratic temperature dependence of dc resistivity is expected as a Fermi-liquid behavior where electron–electron scattering plays a key role in the correlated electron systems at low temperatures.[24,25]

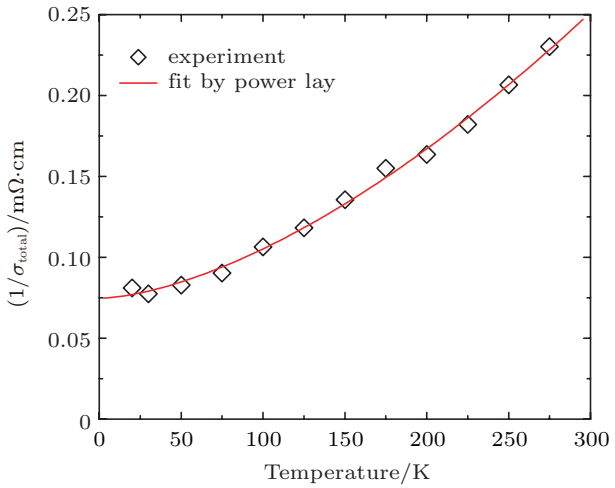


Fig. 4. (color online) The black hollow diamond scatter is the plot of $\rho_{\text{total}}(T)$. The red smooth line through the data is the fit by power law with $n = 1.6$.

In order to study the electronic properties in two subsystems,[12] respectively, we decomposed the optical conductivity in low frequency into two different contributions as our previous fitting (broad Drude and narrow Drude). Firstly, we extract the plasma frequency (Ω_{pb} and Ω_{pn}), and plot them as a function of temperature (shown in Fig. 5(a)). This shows that upon cooling, Ω_{p} is roughly a constant for both two components, indicating that band structure does not change much as the temperature cools down, which is consistent with the previous work.[12] Figure 5(b) shows the plot of scattering rate $1/\tau$, exhibiting a roughly constant $1/\tau_{\text{b}}$, which suggests an incoherent background with T independence of broad Drude component, and quadratic-like $1/\tau_{\text{n}}$, which is responsible for a hidden Fermi-liquid state.

To analyze the narrow Drude component accurately, $\rho_{\text{n}} = 1/\sigma_{\text{n}}(0)$ and $1/\tau$ are extracted, as shown in Fig. 6. This reveals that both ρ_{n} and $1/\tau_{\text{n}}$ exhibit a T-quadratic relationship, indicating a Fermi-liquid behavior in the narrow Drude component.

The decomposition method of two Drude terms and a Lorentz term is widely used in optical spectra analysis of 122 iron pnictides,[12,26,27] because of the multiple band character, which results in two groups of charge carriers with different scattering rates.[28,29] In addition, two superconducting gaps

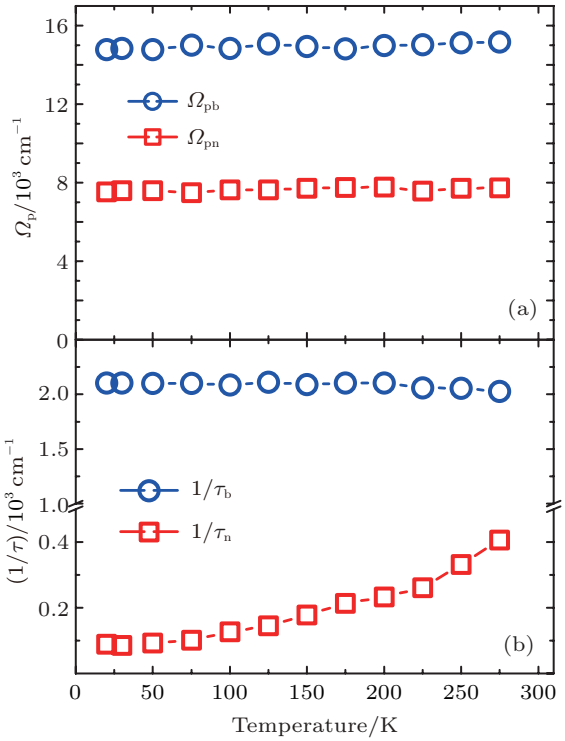


Fig. 5. (color online) The T dependence of (a) the plasma frequency Ω_{p}, (b) the scattering rate $1/\tau$.

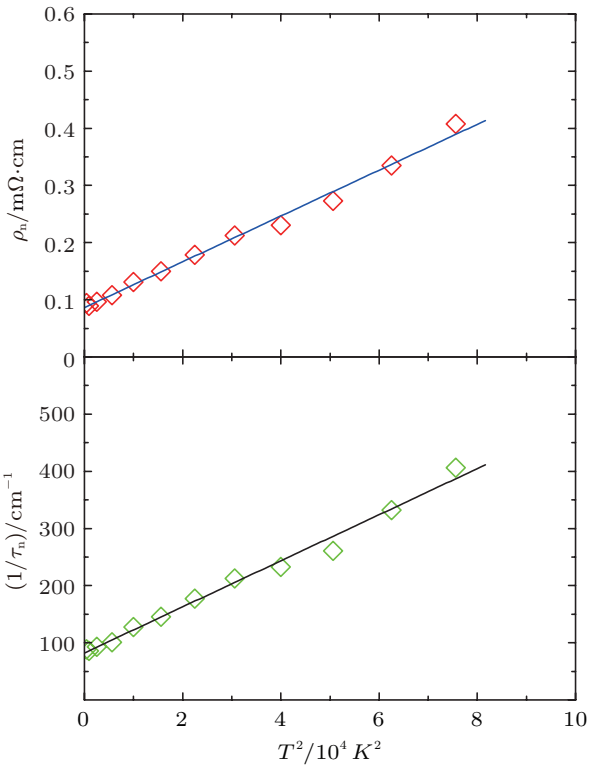


Fig. 6. (color online) (a) The red diamond scatter is the plot of ρ_{n}, with a blue straight fitting line through it. (b) The green diamond scatter is $1/\tau_{\text{n}}$ as a function of T^2, with a black straight fitting line through it.

are fully opened in optimally doped $Ba_{0.6}K_{0.4}Fe_2As_2$,[30] which are obtained by fitting the optical conductivities by two corresponding Mattis–Bardeen terms, indicating that both Drude components contribute to the superconductivity in 122

iron pnictides. It is suggested that the broad Drude term is no longer metallic but is instead incoherent and is appropriate to be described by a bound excitations or a series of bound excitations,[28] because the mean free path $l = v_F\tau$ (v_F is the Fermi velocity) is less than the shortest interatomic spacing, disobeying the Mott–Ioffe–Regel limit.[31–33] Whereas, a T-quadratic $1/\tau$ in narrow Drude term is generally associated with Fermi liquid.[27] Similar temperature dependence can also be found in Ruthenate superconductors,[20] organic layered superconductors,[34] and high-temperature superconductors.[22,31,32] However, it was recently strongly implied that there exists a T-linear scattering rate in optimally doped $Ba_{0.6}K_{0.4}Fe_2As_2$ and $BaFe_2As_{1.4}P_{0.6}$,[26] indicating a non-Fermi-liquid behavior due to the spin fluctuation, which is drastically argued as the media of the pairing of electrons in unconventional superconductors. In spite of this, our results manifest that non-Fermi-liquid behavior is not a universal phenomenon existing in all Ba122 systems, indicating that superconducting state may originate from a Fermi liquid. In a Fermi liquid, electron–electron Umklapp scattering process dominates the scattering rate, which is associated to

$$\hbar/\tau_e(T) = A(k_BT)^2/E_F, \tag{3}$$

where A is a dimensionless constant.[35] Because we have nearly the same $1/\tau_n$ and Fermi energy as in $BaFe_{1.9}Ni_{0.1}As_2$,[27] resulting in a same magnitude $A \approx 1$–2 for our sample, which is consistent with the weak coupling limit and does not indicate any quantum critical behavior.

4. Conclusion

The infrared optical conductivity of $BaFe_{1.904}Ni_{0.096}As_2$ single crystal is obtained from 275 K down to 20 K. A power law fitting of the reciprocal of zero frequency optical conductivity ρ_{total} with $n \neq 2$ indicates a non-Fermi-liquid behavior in the charge carriers of the material. Two Drude terms and a Lorentz term are used for the fitting of optical conductivity for the sake of eliminating the deviation from a single Drude-like response, which is due to the presence of charge carriers with different scattering rate. An incoherent temperature independent $1/\tau_b$ and a T-quadratic $1/\tau_n$ are extracted, which reveal a hidden Fermi-liquid behavior in the $BaFe_{1.904}Ni_{0.096}As_2$ compound.

Acknowledgment

We thank H. Q. Luo and P. C. Dai for providing $BaFe_{1.904}Ni_{0.096}As_2$ crystals.

References

[1] Kamihara Y, Watanabc T, Hirano M and Hosono H 2008 *J. Am. Chem. Soc.* **130** 3296
[2] Chen X H, Wu T, Wu G, Liu R H, Chen H and Fang D F 2008 *Nature* **453** 761
[3] Ren Z A, Lu W, Yang J, Yi W, Shen X L, Li Z C, Che G C, Dong X L, Sun L L, Zhou F and Zhao Z X 2008 *Chin. Phys. Lett.* **25** 2215
[4] Hess C, Kondrat A, Narduzzo A, Hamann-Borrero J E, Klingeler R, Werner J, Behr G and Büchner B 2009 *Europhys. Lett.* **87** 17005
[5] Graser S, Maier T A, Hirschfeld P J and Scalapino D J 2009 *New. J. Phys.* **11** 025016
[6] Rullier-Albenque F, Colson D, Forget A and Alloul H 2009 *Phys. Rev. Lett.* **103** 057001
[7] Singh D J 2008 *Phys. Rev. B* **78** 094511
[8] Mazin I I and Schmalian J 2009 *Physica C* **469** 614
[9] Ma F J, Lu Z Y and Xiang T 2010 arXiv: **0806** 3526v3
[10] Hsieh D, Xia Y, Wray L, Qian D, Gomes K, Yazdani A, Chen G F, Luo J L, Wang N L and Hasan M Z 2008 arXiv: **0812** 2289
[11] Yi M, Lu D H, Analytis J G, Chu J H, Mo S K, He R H, Zhou X J, Chen G F, Luo J L, Wang N L, Hussain Z, Singh D J, Fisher I R and Shen Z X 2009 *Phys. Rev. B* **80** 024515
[12] Wu D, Barišić N, Kallina P, Faridian A, Gorshunov B, Drichko N, Li L J, Lin X, Cao G H, Xu Z A, Wang N L and Dressel M 2010 *Phys. Rev. B* **81** 100512(R)
[13] Löhneysen H, Rosch A, Vojta M and Wölfle P 2007 *Rev. Mod. Phys.* **79** 1015
[14] Monthoux P, Pines D and Lonzarich G G 2007 *Nature* **450** 1177
[15] Moriya T and Ueda K 2000 *Adv. Phys.* **49** 555
[16] Mazin I I, Singh D J, Johannes M D and Du M H 2008 *Phys. Rev. Lett.* **101** 057003
[17] Basov D N and Timusk T 2005 *Rev. Mod. Phys.* **77** 721
[18] Basov D N, Averitt R D, van der Marel D, Dressel M and Haule K 2011 *Rev. Mod. Phys.* **83** 471
[19] Marsik P, Wang C N, Rössle M, Yazdi-Rizi M, Schuster R, Kim K W, Dubroka A, Munzar D, Wolf T, Chen X H and Bernhard C 2013 *Phys. Rev. B* **88** 180508
[20] Homes C C, Reedyk M, Cradles D A and Timusk T 1993 *Appl. Opt.* **32** 2976
[21] Hu W Z, Dong J, Li G, Zheng P, Chen G F, Luo J L and Wang N L 2008 *Phys. Rev. Lett.* **101** 257005
[22] Akrap A, Tu J J, Li L J, Cao G H, Xu Z A and Homes C C 2009 *Phys. Rev. B* **80** 180502
[23] Schafgans A A, Pursley B C, LaForge A D, Sefat A S, Mandrus D and Basov D N 2011 *Phys. Rev. B* **84** 052501
[24] Abrikosov A A, Gor'kov L P and Dsyaloshinskii I Y 1963 *Methods of Quantum Field Theory in Statistical Physics* (Englewood: Prentice-Hall)
[25] Pines D and Nozières P 1966 *The Theory of Quantum Liquids* (Reading: Addison-Wesley)
[26] Dai Y M, Xu B, Shen B, Xiao H, Wen H H, Qiu X G, Homes C C and Lobo R P S M 2013 *Phys. Rev. Lett.* **111** 117001
[27] Barišić N, Wu D, Dressel M, Li L J, Cao G H and Xu Z A 2010 *Phys. Rev. B* **82** 054518
[28] Tu J J, Li J, Liu W, Punnoose A, Gong Y, Ren Y H, Li L J, Cao G H, Xu Z A and Homes C C 2010 *Phys. Rev. B* **82** 174509
[29] Kim K W, Rössle M, Dubroka A, Malik V K, Wolf T and Bernhard C 2010 *Phys. Rev. B* **81** 214508
[30] Dai Y M, Xu B, Shen B, Wen H H, Qiu X G and Lobo R P S M 2013 *Europhys. Lett.* **104** 47006
[31] Mott N F 1972 *Philos. Mag.* **26** 1015
[32] Gurvitch M 1981 *Phys. Rev. B* **24** 7404
[33] Hussey N E, Takenaka K and Takagi H 2004 *Philos. Mag.* **84** 2847
[34] Dressel M and Grüner G 2001 *Electrodynamics of Solids* (Cambridge: Cambridge University Press)
[35] Ashcroft N W and Mermin N D 1976 *Solid State Physics* (Philadelphia: Saunders College Publishing)